

Communication

Carnation-like Morphology of BiVO₄-7 Enables Sensitive Photoelectrochemical Determination of Cr(VI) in the Food and Environment

Wenqin Wu^{1,2,†}, Zhao Tan^{1,2,3,†}, Xiao Chen^{1,2,3}, Xiaomei Chen^{1,2}, Ling Cheng^{1,2}, Huimin Wu³, Peiwu Li^{1,2} and Zhaowei Zhang^{1,2,*} 

- ¹ Key Laboratory of Detection for Mycotoxins, Ministry of Agriculture and Rural Affairs, National Reference Lab for Biotoxin Test, Oil Crops Research Institute of the Chinese Academy of Agricultural Sciences, Wuhan 430062, China; wuwenqin@caas.cn (W.W.); 13476831558@163.com (Z.T.); 202021106010763@stu.hubu.edu.cn (X.C.); chenxiaomei_200870@126.com (X.C.); chengling@caas.cn (L.C.); peiwuli@oilcrops.cn (P.L.)
- ² Key Laboratory of Biology and Genetic Improvement of Oil Crops, Ministry of Agriculture and Rural Affairs, Oil Crops Research Institute of the Chinese Academy of Agricultural Sciences, Wuhan 430062, China
- ³ College of Chemistry and Chemical Engineering, Hubei University, Wuhan 430062, China; whm267@hubu.edu.cn
- * Correspondence: zwzhang@whu.edu.cn; Tel.: +86-27-86711839
- † These authors contributed equally to this work.

Abstract: Hexavalent chromium, namely, Cr(VI), is a significant threat to ecological and food safety. Current detection methods are not sensitive to Cr(VI). A photoelectrochemical (PEC) sensor based on bismuth vanadate (BiVO₄) was developed for sensitive detection of Cr(VI). First, BiVO₄-X (X: the pH of the reaction precursor solution) was synthesized using a facile surfactant-free hydrothermal method. The BiVO₄-X morphology was well controlled according to pH values, showing rock-like (X = 1), wrinkled bark-like (X = 4), carnation-like (X = 7), and the collapsed sheet-like morphologies (X = 9, 12). BiVO₄-7 exhibited excellent photoelectric performance due to a proper band structure under visible light and a large specific surface area. Then, BiVO₄-7 was used to construct a PEC sensor to detect Cr(VI), which was demonstrated to have a low detection limit (10 nM) and wide detection range (2–210 μM). The BiVO₄-7 PEC sensor had a stable output signal, as well as excellent reproducibility, repeatability, and selectivity. We used the BiVO₄-7 PEC sensor to detect Cr(VI) in real environmental and food samples, resulting in a satisfactory recovery of 90.3–103.0%, as determined by comparison with results obtained using a spectrophotometric method. The BiVO₄-7 PEC sensor is promising for practical application to heavy metal detection in the food and environment.

Keywords: photoelectrochemistry; hexavalent chromium; bismuth vanadate; food safety; environmental monitoring



Citation: Wu, W.; Tan, Z.; Chen, X.; Chen, X.; Cheng, L.; Wu, H.; Li, P.; Zhang, Z. Carnation-like Morphology of BiVO₄-7 Enables Sensitive Photoelectrochemical Determination of Cr(VI) in the Food and Environment. *Biosensors* **2022**, *12*, 130. <https://doi.org/10.3390/bios12020130>

Received: 19 January 2022

Accepted: 16 February 2022

Published: 19 February 2022

Publisher's Note: MDPI stays neutral with regard to jurisdictional claims in published maps and institutional affiliations.



Copyright: © 2022 by the authors. Licensee MDPI, Basel, Switzerland. This article is an open access article distributed under the terms and conditions of the Creative Commons Attribution (CC BY) license (<https://creativecommons.org/licenses/by/4.0/>).

1. Introduction

The rapid development of industrial manufacturing has made chromium contamination an increasingly significant focus in the environmental monitoring and food industries [1–3]. With a group I classification from the International Agency for Research on Cancer, hexavalent chromium (Cr(VI)) can cause genotoxic tumors, genetic defects, asthma, and allergies and harm the environment by accumulating in the ambient environment and food chains [4–9]. A sensitive detection method needs to be developed to trace Cr(VI) in the environment and food [10]. Current detection methods include atomic absorption spectrometry [11], fluorescence spectroscopy [12], high-performance liquid chromatography-inductively coupled plasma-mass spectrometry [13], and spectrophotometric methods [14], all of which have considerable sensitivity and accuracy but involve complex and laborious processes, expensive equipment, and dedicated operators [11–13].

A promising technique is the use of a photoelectrochemical (PEC) sensor, which offers the advantages of being low cost, requiring simple equipment that is easy to operate, and a low background signal [15–19]. However, a remaining challenge is to improve PEC detection sensitivity, which can be addressed by two strategies. One is surface modification via nanomaterials, such as BiPO₄/BiOI [20], PbS [21], and TiO₂ [22], for Cr(VI) detection in water samples [21,22]. Among various nanomaterials, scheelite monoclinic BiVO₄ is one of the most promising visible-light-responsive electrode materials due to a wide bandgap, excellent stability, and low toxicity [23] that is widely used in optoelectronics research [24] and a potential nanomaterial for photoelectric detection of the heavy metal Cr(VI). However, bare BiVO₄ has a low electron mobility, rapid photoelectric carrier recombination, and poor adsorption performance, resulting in low photoelectric catalytic performance [25]. Many strategies have been used to overcome these problems, including controlling the morphology [26], doping with metallic or nonmetallic elements [27], and coupling with multiple semiconductors to construct heterojunctions [28]. An alternative strategy, especially for Cr(VI) detection in food and soil samples, is to reduce the sample matrix effect by suitable sample preparation. A water sample is a typical matrix for Cr(VI) detection by a PEC sensor. Sample preparation mainly includes extraction by acid and alkaline solutions. However, sample preparation for Cr(VI) detection in solid agricultural products and food samples is more complex, and an extraction procedure is required to meet recovery requirements.

Odeyl benzene sulfonate (SDBS), polyvinyl pyrrolidone (PVP), cetyltrimethylammonium bromide (CTAB), dodecylamine (DA), oleylamine (OL), and oleic acid (OA) are usually used as surfactants to control the growth of the special shapes nanomaterials by adsorbing on the surface of BiVO₄ nanoparticles. However, adding surfactants makes the operation more complicated. In this study, a hydrothermal method without surfactants (SDBS, CTAB, PVP, DA, OL, OA, etc.) was used to synthesize BiVO₄ with a controlled morphology. Fine optimization of the pH used in the synthesis of BiVO₄ resulted in a carnation-like morphology and excellent photoelectric properties. Then, a PEC sensor was developed, and the sensor stability, repeatability, and selectivity during application were evaluated. The PEC sensor based on the optimized BiVO₄ with a carnation-like morphology was used for Cr(VI) detection in soil, rice, peanut, and water. A simple sample preparation protocol was developed to reduce the complex matrix effect. This PEC sensor can be extensively applied to monitor environmental and food safety.

2. Experiments

2.1. Chemicals and Reagents

The chemicals and reagents used in this study are listed in the Supplementary Material.

2.2. Synthesis and Characterization of BiVO₄

A total of 15 milliliters of 5 mM Bi(NO₃)₃·5H₂O, 15 mL of 5 mM NH₄VO₃, and 5 mL CH₃COOH were mixed for 30 min at room temperature. The final pH of the solution was adjusted to 1, 4, 7, 9, or 12 by adding NaOH (1 M), and the solution was heated to 100 °C for 20 h. The solution was cooled, washed with ethanol and water three times, and dried for 12 h at 80 °C. Finally, the powder samples were calcined at 350 °C for 2 h in a muffle furnace to obtain final samples of BiVO₄-X (X = 1, 4, 7, 9, and 12, where X is the pH of the precursor solution). The crystal structure, photoelectric performance, morphology, valence state, and PEC mechanism of the synthesized materials were characterized via X-ray diffraction (XRD), electrochemical impedance spectroscopy (EIS), scanning electron microscopy (SEM), X-ray photoelectron spectroscopy (XPS), and UV-Vis diffuse reflection spectroscopy (UV-Vis DRS), and the results are provided in the Supporting Materials. Details of the instruments used are also provided in the Supplementary Materials.

2.3. PEC Sensor Preparation

A bare indium tin oxide (ITO) electrode (length: 2 cm, width: 1 cm) was ultrasonicated in acetone, ethanol, and ultrapure water for 10, 10, and 15 min, respectively. Then, 3 mg

of $\text{BiVO}_4\text{-X}$ were dispersed in 0.2 mL of ethanol containing 0.3 mL of chitosan (0.5%), and the dispersion was ultrasonicated for 20 min. Finally, 30 μL of the $\text{BiVO}_4\text{-X}$ dispersion was coated on a treated ITO electrode before use.

2.4. Procedure for Using the PEC Sensor to Detect Cr(VI)

The BiVO_4 -based PEC apparatus is shown in the Supplementary Materials (Figure S1). After Cr(VI) was added to an electrolyte (0.1 M NaSO_4), we immersed the sensor in the solution, and an electrochemical workstation was used to record the current signal with or without light. A correlation curve between the photocurrent signal and the corresponding Cr(VI) concentration was constructed and used to calculate the detection limit and range.

2.5. PEC Sensor Evaluation

A calibration curve was developed to calculate the LOD and linear range. A series of Cr(VI) standard solutions (2, 4, 6, 8, 10, 20, 30, 40, 50, 70, 90, 130, 190, and 210 μM) were used to establish standard curves for Cr(VI). Each data point in the standard curve was the result of three measurements. LODs were calculated using $\text{LOD} = X + 3\text{SD}$, where X is the average concentration determined by 21 repeated experiments on blank samples, and SD is the corresponding standard deviation. Spiked experiments were performed to evaluate the PEC sensor performance in terms of repeatability, reproducibility, stability, selectivity, and applicability to real samples. The repeatability was evaluated through 20 consecutive tests on 50 μM Cr(VI) using looped on-and-off light switching. Nine electrodes were tested to assess the sensor reproducibility for detection of 50 μM Cr(VI). The sensor stability was evaluated by comparing the photocurrent after 33 days with the initial photocurrent. The sensor selectivity was investigated by adding common ions Cl^- , NO_3^- , Fe^{3+} , Cu^{2+} , Co^{2+} , Zn^{2+} , and Na^+ to a 10 μM Cr(VI) solution. A real sample analysis was conducted on spiked samples of real peanut, rice, soil, and tap water samples (spiking concentrations: 10 and 100 μM Cr). Recoveries were calculated by comparing the results obtained using the PEC sensor and flame atomic absorption spectrometry.

2.6. Sample Pretreatment

The samples were pretreated following a certified method (Chinese Environmental Standard: HJ 1082–2019). A 5.0 g solid sample (e.g., soil, rice, or peanut) was extracted using a 50.0 mL mixed solution containing 0.28 M Na_2CO_3 and 0.5 M NaOH , to which 0.08 M MgCl_2 and 0.5 mL of phosphate buffer solution (0.36 M K_2HPO_4 and 0.57 M KH_2PO_4 , pH: 7) were added. The final pH of the filtrate was adjusted to 7.5 before use. The final sample filtrate was added to an electrolyte (0.1 M NaSO_4), and we immersed the PEC sensor in the solution to detect Cr(VI) in real samples.

3. Results and Discussion

3.1. Characterization of $\text{BiVO}_4\text{-X}$

$\text{BiVO}_4\text{-X}$ ($X = 1, 4, 7, 9$, and 12) was synthesized without the use of surfactants. The XRD spectra of $\text{BiVO}_4\text{-X}$ ($X = 1, 4, 7, 9$, and 12) are shown in Figure 1a. $\text{BiVO}_4\text{-7}$ spectrum exhibited peaks at 15.14° , 18.99° , 28.95° , 30.55° , 34.50° , 35.22° , 39.78° , 42.46° , 46.71° , 47.31° , 50.31° , 53.31° , and 58.53° , corresponding to diffraction from the (020), (011), (121), (040), (200), (002), (211), (051), (240), (042), (202), (161), and (321) crystallographic planes of monoclinic BiVO_4 (JCPDS 14-0688). We found that $\text{BiVO}_4\text{-1}$, $\text{BiVO}_4\text{-4}$, and $\text{BiVO}_4\text{-7}$ had the same crystal form, whereas $\text{BiVO}_4\text{-9}$ and $\text{BiVO}_4\text{-12}$ contained $\text{Bi}_{17}\text{V}_3\text{O}_{33}$ (JCPDS 52-1476) due to vanadate hydrolysis.

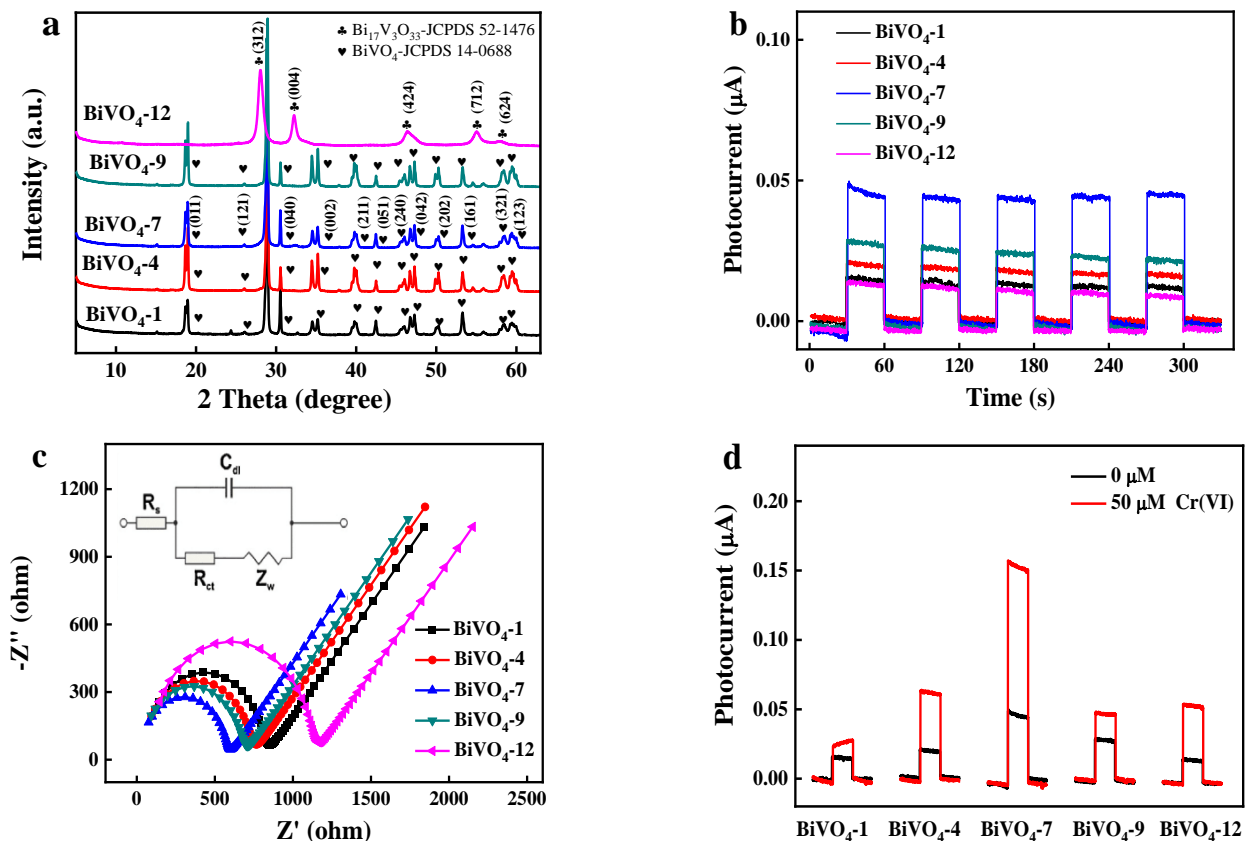


Figure 1. (a) XRD spectra of $\text{BiVO}_4\text{-X}$ ($X = 1, 4, 7, 9,$ and 12); (b) photocurrent responses of $\text{BiVO}_4\text{-X}$ ($X = 1, 4, 7, 9,$ and 12) in 0.1 M NaSO_4 ; (c) EIS spectra of $\text{BiVO}_4\text{-X}$ ($X = 1, 4, 7, 9,$ and 12) in 0.1 M NaSO_4 , where the frequency (Hz) ranges from 1 to 10^6 , and the inset shows the Randles equivalent circuit diagram; (d) photocurrent responses of $\text{BiVO}_4\text{-X}$ ($X = 1, 4, 7, 9,$ and 12) (Cr(VI) : 0 and $50 \mu\text{M}$).

The photoelectric performance of $\text{BiVO}_4\text{-X}$ was preliminarily evaluated via a photoelectric response experiment (Figure 1b) and an EIS test (Figure 1c). A lamp with an irradiation wavelength of 420 nm was switched on and off at 30 s intervals. The highest photocurrent in a 0.1 M NaSO_4 blank electrolyte for $\text{BiVO}_4\text{-X}$ ($X = 1, 4, 7, 9,$ and 12), therefore the highest photoelectric performance was obtained for $\text{BiVO}_4\text{-7}$ (Figure 1b), and the photoelectric performance of the $\text{BiVO}_4\text{-7}$ modified ITO sensor was 500 times higher than that of blank ITO substrates (Supplementary Material S2). The electrochemical performance of $\text{BiVO}_4\text{-X}$ was determined by EIS (Figure 1c). The semicircle diameter is a measure of the charge transfer resistance (R_{ct}). The R_{ct} s of $\text{BiVO}_4\text{-X}$ ($1, 4, 7, 9,$ and 12) were $767, 690, 551, 644,$ and 1041Ω , respectively, where $\text{BiVO}_4\text{-7}$ exhibited the smallest R_{ct} . $\text{BiVO}_4\text{-7}$ exhibited the highest electrochemical performance, both in terms of photoelectric performance and EIS results. A $\text{BiVO}_4\text{-X}$ -based PEC sensor was used to detect Cr(VI) , and the photocurrent responses of $\text{BiVO}_4\text{-X}$ ($X = 1, 4, 7, 9,$ and 12) were recorded (Figure 1d). Among the $\text{BiVO}_4\text{-X}$ ($X = 1, 4, 7, 9,$ and 12) detectors in the presence of $50 \mu\text{M Cr(VI)}$, $\text{BiVO}_4\text{-7}$ showed the maximum photocurrent change and therefore, the highest photoelectric performance for detecting Cr(VI) .

The SEM results showed that fine pH adjustment produced a diversity of morphologies for $\text{BiVO}_4\text{-X}$ ($X = 1, 4, 7, 9,$ and 12). $\text{BiVO}_4\text{-1}$ exhibited an irregular rock-like morphology (Figure S2a,b), and $\text{BiVO}_4\text{-4}$ had the appearance of wrinkled bark (Figure S2c,d). Under neutral conditions, $\text{BiVO}_4\text{-7}$ (Figure 2a,b) had a carnation-like structure assembled from regular sheets. Increasing the pH during $\text{BiVO}_4\text{-X}$ synthesis caused the sheet-like assembly structure to collapse (Figure S2e–h). Combining this result with the photocurrent responses of $\text{BiVO}_4\text{-X}$ showed that the largest current was obtained for the carnation-like morphology due to its uniqueness and increased surface area.

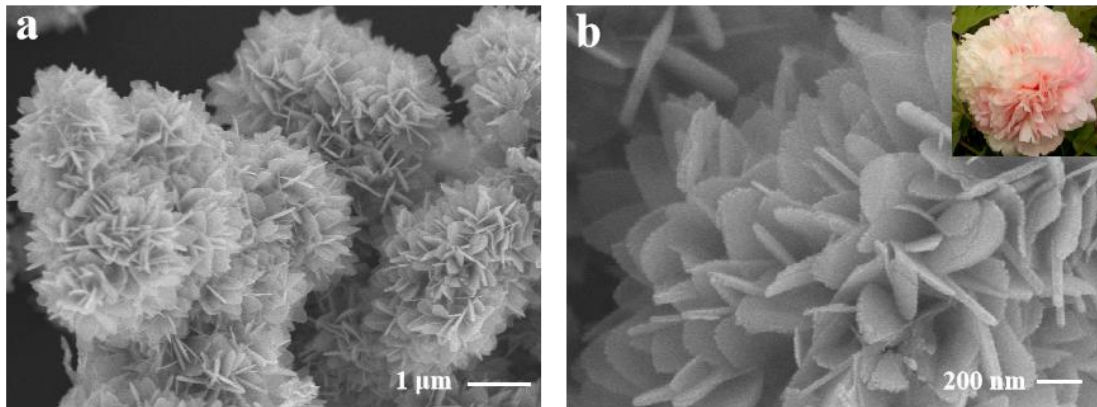


Figure 2. (a) SEM image of BiVO_4 -7 and (b) corresponding high-magnification image.

The valence state and surface chemical composition of BiVO_4 -7 were characterized by XPS. The survey spectrum confirmed the presence of V, Bi, and O in BiVO_4 -7 (Figure 3a). The peaks at 163.7 and 158.4 eV were attributed to the spin-orbit splitting of Bi $4f_{5/2}$ and Bi $4f_{7/2}$, respectively (Figure 3b). The 5.3 eV spacing between the Bi $4f_{5/2}$ and Bi $4f_{7/2}$ peaks indicated a +3 valence state of Bi for an isotype heterojunction sample, as has been previously reported [29].

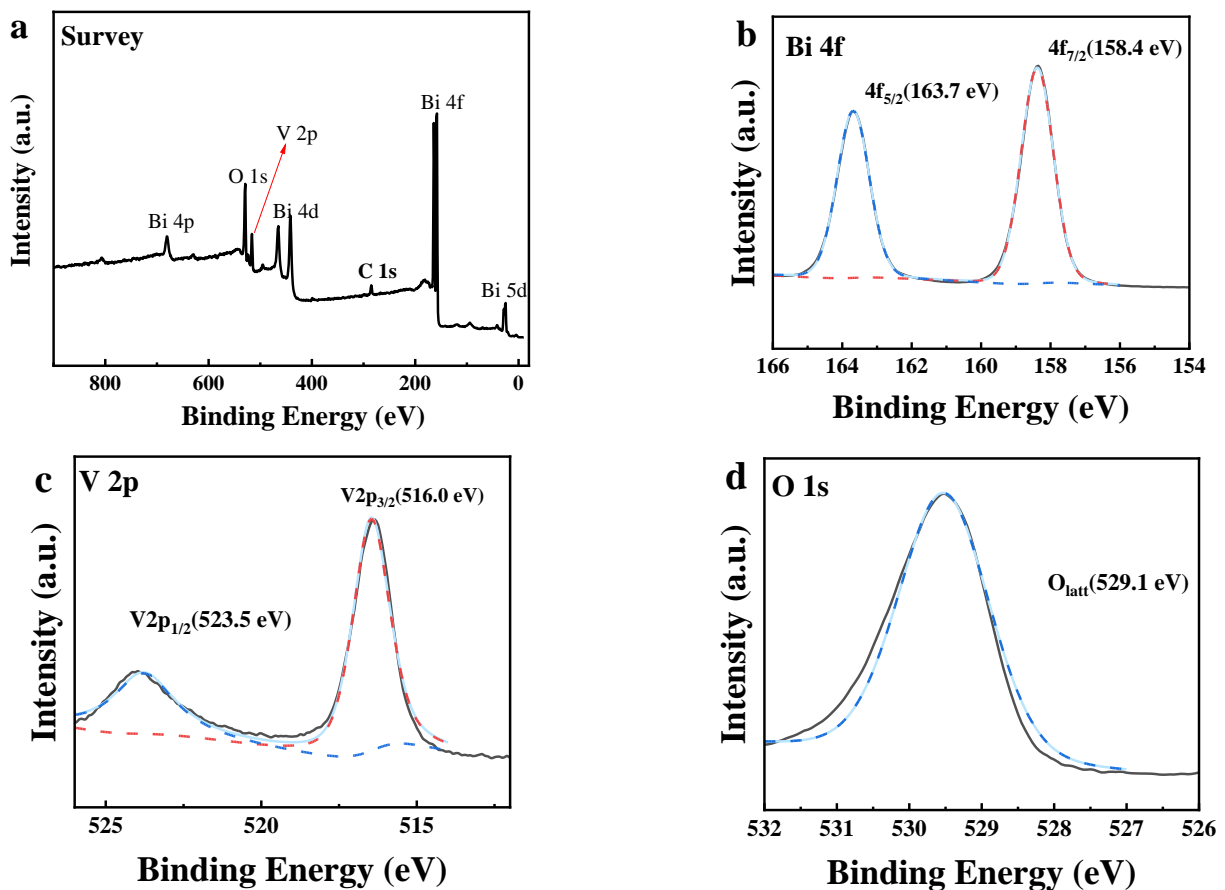


Figure 3. (a) XPS survey spectrum of BiVO_4 -7 and the corresponding high-resolution XPS spectra of (b) Bi 4f, (c) V 2p, and (d) O 1s.

The two characteristic peaks at 523.5 eV and 516.0 eV correspond to V $2p_{1/2}$ and V $2p_{3/2}$, respectively (Figure 3c). The 7.5 eV spacing between the peaks of $2p_{1/2}$ and V $2p_{3/2}$ confirmed the +5 valence state of vanadium. The peak in the high-resolution XPS

spectrum at 529.1 eV (O 1s) was attributed to BiVO₄-7 lattice oxygen (O_{latt}) (Figure 3d). The XPS characterization results indicated that BiVO₄-7 was completely pure.

BiVO₄-7 showed strong absorption in the visible range, indicating good optical performance (Figure 4a). The BiVO₄-7 bandgaps were estimated using the formula $\alpha h\nu = A (h\nu - E_g)^n$ (E_g : bandgap; A: a constant; ν : light frequency; α : absorption coefficient). BiVO₄ had an n of 1/2 [30], and plots of $(\alpha h\nu)^2$ versus the photon energy ($h\nu$) were used to estimate the gap energy (E_g) for BiVO₄-7 of 2.45 eV (Figure 4b). The optical band structure of BiVO₄-7 was calculated based on the PEC mechanism. The energies of the conduction band (CB) and valence band (VB) of BiVO₄-7 were estimated using the following formulae.

$$E_{CB} = X - E_c - 0.5 E_g \quad (1)$$

$$E_{VB} = E_{CB} + E_g \quad (2)$$

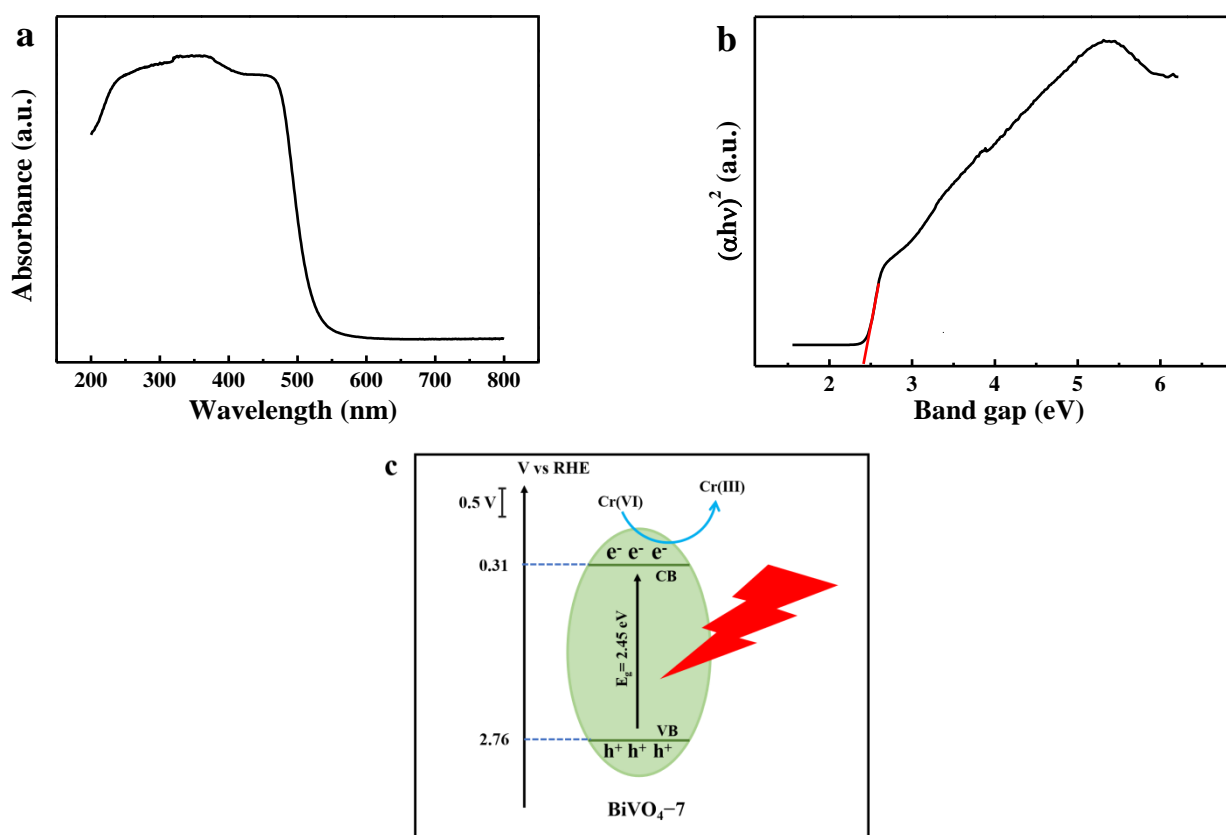


Figure 4. (a) UV-Vis diffuse reflectance spectra for BiVO₄-7; (b) plots of $(\alpha h\nu)^2$ vs. the photon energy ($h\nu$) for BiVO₄-7; (c) photoelectrochemical mechanism for Cr(VI) detection by BiVO₄-7.

E_c denotes the energy of free electrons on the hydrogen scale. This value was approximately 4.5 eV, and the electronegativity (X) of BiVO₄ was 6.035 eV [31]. The formula presented above was used to calculate the E_{CB} and E_{VB} of BiVO₄-7 as 0.31 and 2.76 eV, respectively. Under visible light irradiation, BiVO₄-7 generated hole-electron pairs (h^+/e^-) that reduced Cr(VI) to Cr(III) and changed the photocurrent (Figure 4c).

3.2. Photoelectrochemical Detection of Cr(VI)

An ultrasensitive BiVO₄-7 PEC sensor was developed to detect Cr(VI). The PEC response of the BiVO₄-7 sensor to different Cr(VI) concentrations is shown in Figure 5a. The photocurrent increased significantly with the chromium concentration because the reduction of Cr(VI) to Cr(III) accelerated electron transfer. The regression equation for the corresponding logarithmic calibration curve (Figure 5b) was $\Delta I = -0.005 + 0.123 \log c$, with a

correlation coefficient of 0.994. Here, c represents the Cr(VI) concentration, and $\Delta I = I - I_0$, where I and I_0 represent the photocurrent and dark current, respectively. The relation between ΔI and the Cr(VI) concentration was highly linear in the range of 2–210 μM , and the limit of detection (LOD, $S/N = 3$) was deduced to be 0.01 μM . Compared to previous reports, the LODs of the proposed PEC sensor were 10–200 fold lower and the linear range was wider due to the use of $\text{BiVO}_4\text{-7}$ (Table 1).

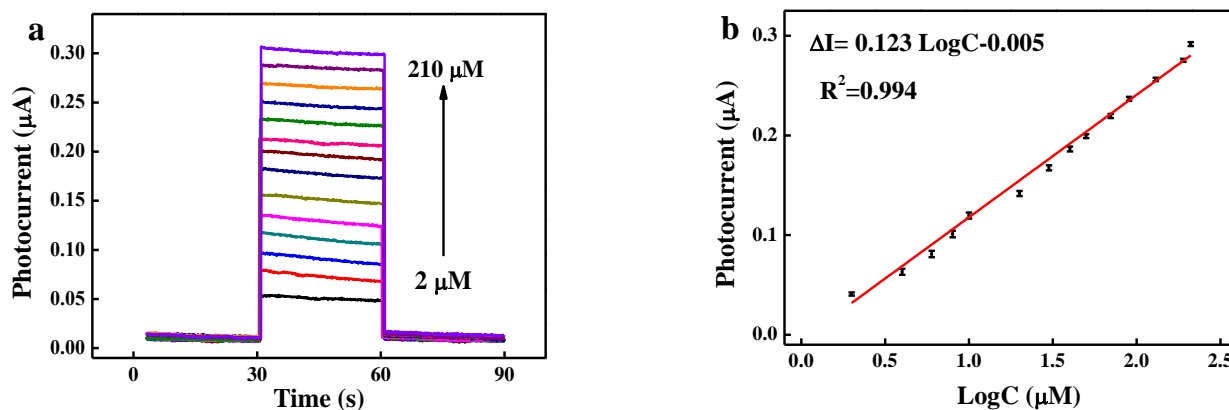


Figure 5. (a) Photocurrent response curve and (b) corresponding calibration curve for detection of different concentrations of Cr (VI) (2 to 210 μM) using $\text{BiVO}_4\text{-7}$.

Table 1. Comparison between the performance of the proposed PEC sensor and reported results for Cr(VI) detection.

Materials	Technique	Linear Range (μM)	LOD (μM)	Ref.
GCPF	Fluorescence	0–50	0.22	[32]
GA-AuNPs	Colorimetry	2–20	2.0	[33]
Pd/Ti	DPV	19–100	0.1	[34]
SQDs	Fluorescence	10–120	0.36	[35]
CDs/ C_3N_4	Fluorescence	2–80	0.39	[36]
CDs@Eu-MOFs	Fluorescence	2–100	0.21	[37]
$\text{BiVO}_4\text{-7}$	PEC	2–210	0.01	This work

GA-AuNPs: gallic acid capped gold nanoparticles; DPV: differential pulse voltammetry; SQDs: sulfur quantum dots; CDs: carbon dots; GCPF: glutaraldehyde cross-linked chitosan polymer fluorophores; CDs@Eu-MOFs: nitrogen and cobalt (II) co-doped carbon dots encapsulated in europium metal–organic frameworks.

3.3. Repeatability, Reproducibility, Stability, and Selectivity of the $\text{BiVO}_4\text{-7}$ Sensor

Twenty consecutive on/off switching loops of the light attenuated the photocurrent intensity by less than 10% for 50 μM Cr(VI) and a 0.4 V bias voltage (Figure 6a), demonstrating excellent repeatability for the $\text{BiVO}_4\text{-7}$ PEC sensor. A relative standard deviation (RSD) of 2.24% was determined using nine electrodes to detect 50 μM Cr(VI), showing the high reproducibility of the $\text{BiVO}_4\text{-7}$ PEC sensor (Figure 6b).

In a long-term stability experiment lasting 33 days, 94.6% of the initial photocurrent of $\text{BiVO}_4\text{-7}$ was retained (Figure 6c). A detection specificity experiment was performed by adding a tenfold concentration of interfering ions (Cl^- , NO_3^- , Fe^{3+} , Cu^{2+} , Co^{2+} , Zn^{2+} , and Na^+) to 10 μM hexavalent chromium in an electrolyte. The results demonstrated the photocurrent was retained in the presence of the spiked interfering ions (Figure 6d), indicating that the $\text{BiVO}_4\text{-7}$ PEC sensor had excellent selectivity.

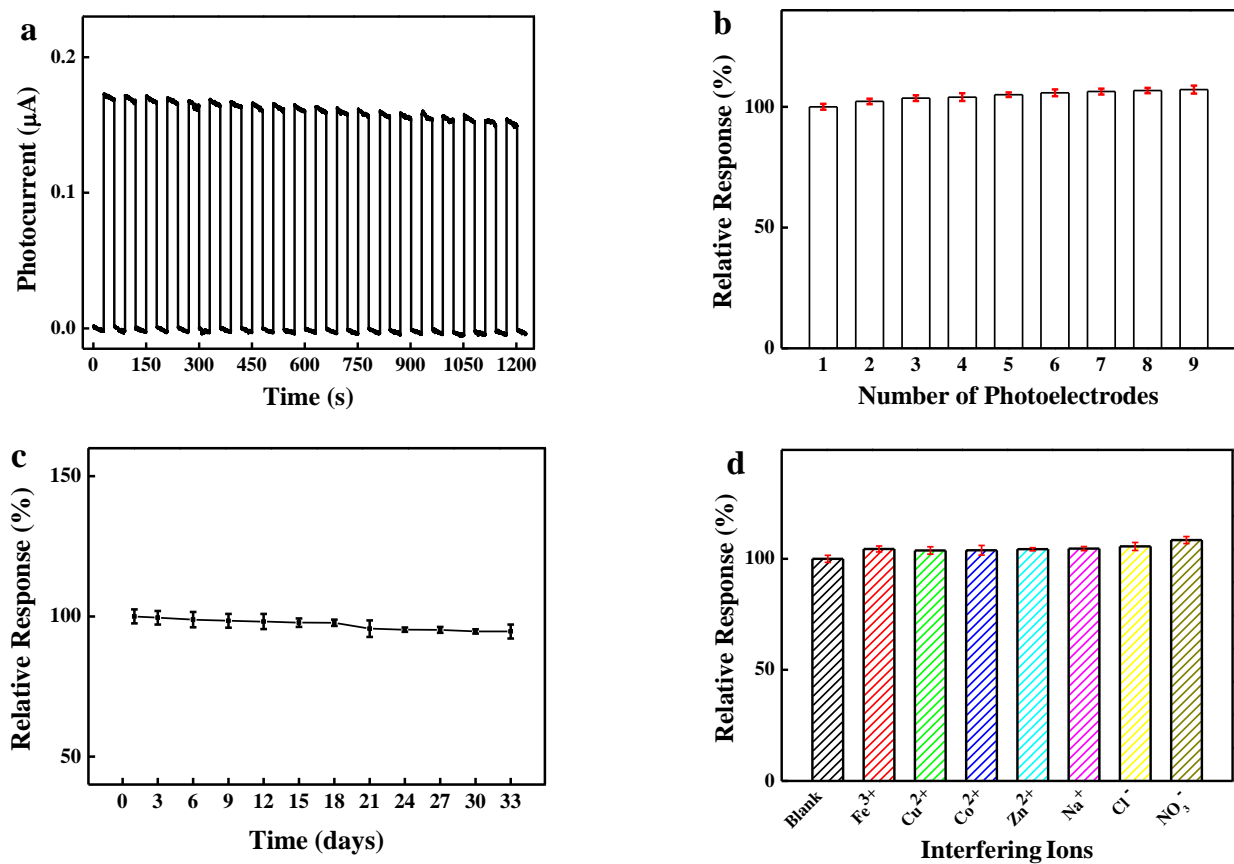


Figure 6. (a) The repeatability (short-term stability) for 20 consecutive tests for 50 mM Cr(VI) under a 0.4 V bias voltage; (b) reproducibility based on nine parallel photoelectrodes; (c) long-term stability, and (d) selectivity of the BiVO₄-7 sensor.

3.4. Real Sample Analysis

The BiVO₄-7 PEC sensor was used to detect Cr(VI) in peanut, rice, soil, and tap water samples to validate the sensor applicability. We spiked real samples with 10 and 100 µM Cr(VI) and obtained good recoveries of 90.3–103% with RSDs less than 8.39% (Table 2). The results indicated that the BiVO₄-7 PEC sensor could be used for Cr(VI) detection in environmental and food safety monitoring.

Table 2. Cr(VI) detection results for a real sample using the PEC sensor (n = 3).

Samples	Original	Added (µM)	Found (µM)	RSD (%)	Recovery (%)	Flame Atomic Absorption Spectrometry (µM)
Peanut	Not found	10	9.90	2.36	99.0	9.93
		100	96.3	3.37	96.3	97.0
Rice	Not found	10	9.41	2.44	94.1	9.45
		100	97.2	2.57	97.2	98.0
Soil	Not found	10	9.26	4.04	92.6	9.30
		100	90.3	8.39	90.3	91.0
Tap water	Not found	10	9.38	1.22	93.8	9.28
		100	103.0	3.87	103.0	101.2

4. Conclusions

In summary, we synthesized BiVO₄ (BiVO₄-7) with a carnation-like morphology by fine pH adjustment without the use of a surfactant. The unique morphology and high specific surface area of the BiVO₄-7 PEC sensor resulted in high performance for Cr(VI)

detection, with a wide linear range of 2–210 μM and a low LOD of 0.01 μM . This PEC sensor exhibited outstanding repeatability (20 times), long-term stability over 33 days, excellent reproducibility, and selectivity. Moreover, the PEC sensor showed excellent accuracy for Cr(VI) detection in peanuts, rice, soil, and tap water, with satisfactory recovery rates of 90.3 to 103.0%. This BiVO_4 -7 based PEC sensor has broad potential in environmental and food safety monitoring.

Supplementary Materials: The following supporting information can be downloaded at: <https://www.mdpi.com/article/10.3390/bios12020130/s1>, Figure S1. The real picture of the PEC sensor: (A) the detection instrument of the PEC sensor; (B) the three-electrode system. Figure S2. SEM images of (a, b) BiVO_4 -1, (c, d) BiVO_4 -4, (e, f) BiVO_4 -9, and (g, h) BiVO_4 -12.

Author Contributions: W.W.: methodology, investigation, writing—original draft; Z.T.: formal analysis, writing—original draft; X.C. (Xiao Chen): data curation; X.C. (Xiaomei Chen): resources; L.C.: validation; H.W.: validation; P.L.: project funding acquisition; Z.Z.: conceptualization, methodology, writing—review and editing, supervision, project funding acquisition. All authors have read and agreed to the published version of the manuscript.

Funding: This research was funded by the National Natural Science Foundation of China, grant number 32072331, 32102084, and the Science and Technology Project of Tibet Autonomous Region, China, grant number XZ202102YD0033C.

Institutional Review Board Statement: Not applicable.

Informed Consent Statement: Not applicable.

Conflicts of Interest: The authors declare no competing interest.

References

1. Shellaiah, M.; Sun, K.W. Diamond-based electrodes for detection of metal ions and anions. *Nanomaterials* **2021**, *12*, 64. [[CrossRef](#)] [[PubMed](#)]
2. Wang, K.; He, H.; Li, D.; Li, Y.; Li, J.; Li, W.Z. Photoelectrochemical reduction of Cr (VI) on plate-like $\text{WO}_3/\text{BiVO}_4$ composite electrodes under visible-light irradiation: Characteristics and kinetic study. *J. Photochem. Photobiol. A* **2018**, *367*, 438–445. [[CrossRef](#)]
3. Liu, T.; Chu, Z.; Jin, W. Electrochemical mercury biosensors based on advanced nanomaterials. *J. Mater. Chem. B* **2019**, *7*, 3620–3632. [[CrossRef](#)]
4. Almeida, D.S.; Cardoso, R.F.; Tavares, T.; Tito, V.; Carlos, P. Chromium removal from contaminated waters using nanomaterials—A review. *TrAC Trends Anal. Chem.* **2019**, *118*, 277–291. [[CrossRef](#)]
5. Wang, Y.; Ma, J.-X.; Zhang, Y.; Xu, N.; Wang, X.-L. A series of cobalt-based coordination polymer crystalline materials as highly sensitive electrochemical sensors for detecting Trace Cr(VI), Fe(III) Ions, and ascorbic acid. *Cryst. Growth Des.* **2021**, *21*, 4390–4397. [[CrossRef](#)]
6. Yu, Y.; Xue, S.; Zhao, C.; Barnych, B.; Sun, G. Highly sensitive, selective, and reusable nanofibrous membrane-based carbon polymer dots sensors for detection of Cr(VI) in water. *Appl. Surf. Sci.* **2022**, *582*, 152392. [[CrossRef](#)]
7. Zhang, J.F.; Li, S.L. Sensors for detection of Cr(VI) in water: A review. *Int. J. Environ. Anal. Chem.* **2021**, *101*, 1051–1073. [[CrossRef](#)]
8. Pachkawade, V.; IEEE, M. State-of-the-Art in Mode-Localized MEMS coupled resonant sensors: A comprehensive review. *IEEE Sens. J.* **2021**, *21*, 8751–8779. [[CrossRef](#)]
9. Kar, A.; Dey, S.; Burman, D.; Santra, S.; Guha, P.K. RGO/Ni 2O_3 heterojunction-based reusable, flexible device for Cr(VI) ion detection in water. *IEEE Trans. Electron. Devices* **2021**, *68*, 780–785. [[CrossRef](#)]
10. Yatera, K.; Morimoto, Y.; Ueno, S.; Noguchi, S.; Kawaguchi, F.; Tanaka, H.; Suzuki, T. Cancer risks of hexavalent chromium in the respiratory tract. *J. UOEH* **2018**, *40*, 157–172. [[CrossRef](#)]
11. Duran, A.; Tuzen, M.; Soylak, M. Speciation of Cr(III) and Cr(VI) in geological and water samples by ytterbium(III) hydroxide coprecipitation system and atomic absorption spectrometry. *Food Chem. Toxicol.* **2011**, *49*, 1633–1637. [[CrossRef](#)] [[PubMed](#)]
12. Liu, P.; Ptacek, C.J.; Blowes, D.W.; Finrock, Y.Z.; Liu, Y. Characterization of chromium species and distribution during Cr(VI) removal by biochar using confocal micro-X-ray fluorescence redox mapping and X-ray absorption spectroscopy. *Environ. Int.* **2020**, *134*, 105216. [[CrossRef](#)] [[PubMed](#)]
13. Saraiva, M.; Chekri, R.; Leufroy, A.; Guérin, T.; Sloth, J.J.; Jitaru, P. Development and validation of a single run method based on species specific isotope dilution and HPLC-ICP-MS for simultaneous species interconversion correction and speciation analysis of Cr(III)/Cr(VI) in meat and dairy products. *Talanta* **2021**, *222*, 121538. [[CrossRef](#)]
14. James, M.E.; Robert, J.J.; Peter, A.L.; Anthony, D.S. Response of chromium(V) to the diphenylcarbazide spectrophotometric method for the determination of chromium(VI). *Anal. Chrmrca Acta* **1991**, *255*, 31–33.

15. Chen, G.; Wang, H.J.; Wei, X.Q.; Wu, Y.; Gu, W.L.; Hu, L.Y.; Xu, D.C.; Zhu, C.Z. Efficient Z-Scheme heterostructure based on $\text{TiO}_2/\text{Ti}_3\text{C}_2\text{T}'/\text{Cu}_2\text{O}$ to boost photoelectrochemical response for ultrasensitive biosensing. *Sens. Actuators B Chem.* **2020**, *312*, 127951. [[CrossRef](#)]
16. Song, M.; Sun, H.; Yu, J.; Wang, Y.; Li, M.; Liu, M.; Zhao, G. Enzyme-free molecularly imprinted and graphene-functionalized photoelectrochemical sensor platform for pollutants. *ACS Appl. Mater. Interfaces* **2021**, *13*, 37212–37222. [[CrossRef](#)] [[PubMed](#)]
17. Gao, B.; Zhao, Z.; Liang, Z.; Wu, W.; Wang, D.; Han, L. Niu. CdS/ TiO_2 Nanocomposite-based photoelectrochemical sensor for a sensitive determination of nitrite in principle of etching reaction. *Anal. Chem.* **2021**, *93*, 820–827. [[CrossRef](#)]
18. Guo, L.; Yin, H.; Xu, M.; Zheng, Z.; Fang, X.; Chong, R.; Zhou, Y.; Xu, L.; Xu, Q.; Li, J.; et al. In situ generated plasmonic silver nanoparticle-sensitized amorphous titanium dioxide for ultrasensitive photoelectrochemical sensing of formaldehyde. *ACS Sens.* **2019**, *4*, 2724–2729. [[CrossRef](#)]
19. Jalali, M.; Moakhar, R.S.; Abdelfattah, T.; Filine, E.; Mahshid, S.S.; Mahshid, S. Nanopattern-assisted direct growth of peony-like 3D MoS_2/Au composite for nonenzymatic photoelectrochemical sensing. *ACS Appl. Mater. Interfaces* **2020**, *12*, 7411–7422. [[CrossRef](#)]
20. Li, M.; Zhang, G.X.; Feng, C.Q.; Wu, H.M.; Mei, H. Highly sensitive detection of chromium (VI) by photoelectrochemical sensor under visible light based on Bi SPR-promoted $\text{BiPO}_4/\text{BiOI}$ heterojunction. *Sens. Actuators B Chem.* **2020**, *305*, 127449. [[CrossRef](#)]
21. Wang, P.; Cao, L.; Wu, Y.; Di, J. A cathodic photoelectrochemical sensor for chromium(VI) based on the use of PbS quantum dot semiconductors on an ITO electrode. *Mikrochim. Acta* **2018**, *185*, 356. [[CrossRef](#)]
22. Moakhar, R.S.; Goh, G.K.L.; Dolati, A.; Ghorbani, M. Sunlight-driven photoelectrochemical sensor for direct determination of hexavalent chromium based on Au decorated rutile TiO_2 nanorods. *Appl. Catal. B Environ.* **2017**, *201*, 411–418. [[CrossRef](#)]
23. Meng, Q.; Zhang, B.; Fan, L.; Liu, H.; Valvo, M.; Edström, K.; Cuartero, M.; De Marco, R.; Crespo, G.A.; Sun, L. Efficient BiVO_4 photoanodes by postsynthetic treatment: Remarkable improvements in photoelectrochemical performance from facile borate modification. *Angew. Chem. Int. Ed.* **2019**, *58*, 19027–19033. [[CrossRef](#)]
24. Lu, H.; Andrei, V.; Jenkinson, K.J.; Regoutz, A.; Li, N.; Creissen, C.E.; Wheatley, A.E.; Hao, H.; Reisner, E.; Wright, D.S.; et al. Single-source bismuth (Transition Metal) polyoxovanadate precursors for the scalable synthesis of doped BiVO_4 photoanodes. *Adv. Mater.* **2018**, *30*, 1804033. [[CrossRef](#)]
25. Phanichphant, S.; Nakaruk, A.; Chansaenpak, K.; Channei, D. Evaluating the photocatalytic efficiency of the BiVO_4/rGO photocatalyst. *Sci. Rep.* **2019**, *9*, 16091. [[CrossRef](#)]
26. Chen, Y.-S.; Lin, L.-Y.; Chen, X.; Zhou, J.B.; Zhang, T.L.; Ding, L.D. Novel synthesis of highly ordered BiVO_4 nanorod array for photoelectrochemical water oxidation using a facile solution process. *J. Power Sources* **2019**, *436*, 226842. [[CrossRef](#)]
27. Chen, X.; Zhou, J.; Zhang, T.; Ding, L. Enhanced degradation of tetracycline hydrochloride using photocatalysis and sulfate radical-based oxidation processes by Co/BiVO_4 composites. *J. Water Process. Eng.* **2019**, *32*, 100918. [[CrossRef](#)]
28. Li, X.; Jia, M.L.; Lu, Y.T.; Li, N.; Zheng, Y.Z.; Tao, X.; Huang, M.L. $\text{Co}(\text{OH})_2/\text{BiVO}_4$ photoanode in tandem with a carbon-based perovskite solar cell for solar-driven overall water splitting. *Electrochim. Acta* **2020**, *330*, 135183. [[CrossRef](#)]
29. Lin, L.; Xie, Q.; Zhang, M.; Liu, C.; Zhang, Y.; Wang, G.; Zou, P.; Zeng, J.; Chen, H.; Zhao, M. Construction of Z-scheme $\text{Ag-AgBr}/\text{BiVO}_4/\text{graphene}$ aerogel with enhanced photocatalytic degradation and antibacterial activities. *Colloids Surf. A Physicochem. Eng. Asp.* **2020**, *601*, 124978. [[CrossRef](#)]
30. Sajid, M.M.; Khan, S.B.; Shad, N.A.; Amin, N.; Zhang, Z.J. Visible light assisted photocatalytic degradation of crystal violet dye and electrochemical detection of ascorbic acid using a $\text{BiVO}_4/\text{FeVO}_4$ heterojunction composite. *RSC Adv.* **2018**, *8*, 23489–23498. [[CrossRef](#)]
31. Fakhravar, S.; Farhadian, M.; Tangestaninejad, S. Excellent performance of a novel dual Z-scheme $\text{Cu}_2\text{S}/\text{Ag}_2\text{S}/\text{BiVO}_4$ heterostructure in metronidazole degradation in batch and continuous systems: Immobilization of catalytic particles on $\alpha\text{-Al}_2\text{O}_3$ fiber. *Appl. Surf. Sci.* **2020**, *505*, 144599. [[CrossRef](#)]
32. Song, J.; Zhou, H.; Gao, R.; Zhang, Y.; Zhang, H.; Zhang, Y.; Wang, G.; Wong, P.K.; Zhao, H. Selective determination of Cr(VI) by glutaraldehyde cross-linked chitosan polymer fluorophores. *ACS Sens.* **2018**, *3*, 792–798. [[CrossRef](#)]
33. Dong, C.; Wu, G.; Wang, Z.; Ren, W.; Zhang, Y.; Shen, Z.; Li, T.; Wu, A. Selective colorimetric detection of Cr(III) and Cr(VI) using gallic acid capped gold nanoparticles. *Dalton Trans.* **2016**, *45*, 8347–8354. [[CrossRef](#)]
34. Aguirre, M.D.C. Nucleation and growth mechanisms of palladium, nanoflower-shaped, and its performance as electrocatalyst in the reduction of Cr(VI). *J. Appl. Electrochem.* **2019**, *49*, 795–809. [[CrossRef](#)]
35. Tan, Q.; An, X.; Pan, S.; Liu, H.; Hu, X. Hydrogen peroxide assisted synthesis of sulfur quantum dots for the detection of chromium (VI) and ascorbic acid. *Spectrochim. Acta Part A Mol. Biomol. Spectrosc.* **2021**, *247*, 119122. [[CrossRef](#)]
36. Zheng, X.; Ren, S.; Gai, Q.; Liu, W. Carbon dot/carbon nitride composites fluorescent probe for the highly selective detection of Cr(VI) ions. *J. Photochem. Photobiol. A Chem.* **2020**, *400*, 112711. [[CrossRef](#)]
37. Wang, Y.; He, J.; Zheng, M.; Qin, M.; Wei, W. Dual-emission of Eu based metal-organic frameworks hybrids with carbon dots for ratiometric fluorescent detection of Cr(VI). *Talanta* **2019**, *191*, 519–525. [[CrossRef](#)]